

(Invited Paper)

Monolithically Integrated InGaAsP/InP Laser/Modulator Using Identical Layer Approach for Opto-Electronic Oscillator

Chi Wu, Sam Keo, Steve X. Yao, Tasha E. Turner, Larry Davis, Martin G. Young,
Lute Maleki and Siamak Forouhar

Center for Space Microelectronics Technology
Jet Propulsion Laboratory, California Institute of Technology
4800 Oak Grove Drive, Pasadena, CA 91109, USA

ABSTRACT

The microwave optoelectronic oscillator (OEO) has been demonstrated on a breadboard. The future trend is to integrate the whole OEO on a chip, which requires the development of high power and high efficiency integrated photonic components. In this paper, we will present the design and fabrication of an integrated semiconductor laser/modulator using the identical active layer approach on InGaAsP/InP material. The best devices have threshold currents of 50-mA at room temperature for CW operation. The device length is approximately 3-mm, resulting in a mode spacing of 14 GHz. For only 5-dBm microwave power applied to the modulator section, modulation response with 30dB resonate enhancement has been observed. This work shows the promise for an on-chip integrated OEO.

Keywords: Laser, Modulator, Mode-locked lasers, microwave generation, Opto-electronic oscillator, RF Photonics, Integrated Optics, OEIC

I. INTRODUCTION

The opto-electronic oscillator (OEO) [1,2] is a new class of oscillators for generating high spectral purity, high frequency, and high stability RF signals and optical sub-carriers with potentially broad applications in spacecraft communications, fiber/wireless communication systems, and photonic analog-to-digital conversion systems. The lowest phase noise oscillator free running at room temperature has been demonstrated based on OEO configuration with a phase noise of -140 dBc/Hz at 10 kHz away from the carrier frequency of 10GHz [3]. The system consisted of a diode pumped Nd:YAG laser, a LiNbO₃ external modulator, two fiber delay lines, a photo-detector, a microwave/RF amplifier and an RF filter. The whole system was constructed on a 30cm x 40cm breadboard with microwave components occupying the majority of the space. The key step toward an on-chip integrated OEO is to the development of high optical power and efficiency integrated photonic components which can eventually eliminates the need for bulky microwave components.

The diode pumped YAG laser and the LiNbO₃ external modulator could be replaced by distributed feedback (DFB) laser and an integrated electro-absorption modulator to reduce the size and cost. However, even the DFB lasers are too costly for many applications. X.S. Yao and L. Maleki recently demonstrated [4] a coupled opto-electronic oscillator (COEO) in which a multi-mode ring laser was used. Unlike the original OEOs in which the optical oscillation of the pump laser is isolated from the electronic oscillation, in a COEO, the laser oscillation is directly coupled with the electronic oscillation. The coupling of the microwave and optical oscillations causes the laser to mode-lock, and generates stable optical pulses and microwave signals simultaneously. Based on the same operating principle of [4], we believe that a multi-mode Fabry-Perot laser can also be used to construct a COEO. The use of a semiconductor Fabry-Perot laser for COEO could lead to the realization of a compact and low cost COEO in the near future.

In this paper, we present the design, fabrication and characterization of a high power and high efficiency laser/modulator pair integrated in a Fabry-Perot cavity for this application.

II. DEVICE STRUCTURE AND PRINCIPLE OF OPERATION

The preliminary goal is to develop an integrated COEO at ~ 15 GHz. The identical active layer (IAL) approach [5-8] is chosen for the following advantages: (a) simple fabrication process, (b) no material re-growth required, and (c) low modulation voltage. Since the mode spacing is inversely proportional to the cavity length, a device length of about 3-mm is required for a resulting mode spacing of ~ 15 GHz. However, optimization of the device structure is required to achieve low threshold and high power operation for a laser with such a long active cavity.

The device structure of the ILM and its application as an opto-electronic oscillator are shown in Figure 1. The laser/modulator cavity is formed with two regions electrically isolated by a gap of about 10- μ m. The laser cavity is provided by the two cleaved facets, on the gain side, and on the modulator side respectively. Light from the output end of the laser is butt coupled to a single-mode fiber and is detected by a photodetector, amplified by an RF amplifier, filtered by an RF band-pass filter centered around the resonant frequency of the laser (about 14 GHz), and is finally coupled to the RF modulation port of the modulator to form an opto-electronic feedback loop. Just like an OEO, when the gain of the feedback loop is larger than one, an opto-electronic (O/E) oscillation will start. As described in [4], the interaction between the optical oscillation modes and the O/E oscillation modes will force the laser to mode-lock. The mode-locked laser will in turn reinforce the O/E oscillation.

The integrated laser/modulator was grown by Metal Organic Chemical Vapor Deposition (MOCVD). The growth sequence is as follows: an N⁺ InP buffer layer was first grown on the N⁺ InP substrate, followed by a 100-nm thick InGaAsP quaternary lower cladding layer with bandgap wavelength of 1.12 μ m. The active layer consists of four compressive strained (+1%) InGaAsP quantum wells with lattice matched InGaAsP ($\lambda_g=1.12$ μ m) barriers. A symmetric InGaAsP ($\lambda_q=1.12$ μ m) upper cladding layer was then grown on the top of active layer and followed by p-InP cladding layers. Two etch-stops were embedded in the P-InP cladding layer for the accurate control of the ridge depth and isolation groove. Finally, a p⁺ InGaAs layer (0.2 μ m) was grown for ohmic contact.

The wafer was further processed in the following four steps:

- (1) An ohmic contact metal layer was first deposited on the p⁺ InGaAs layer. A gap between the laser and modulator sections was defined.
- (2) A 2.5 μ m ridge was etched using photoresist as a mask.
- (3) After formation of the ridge, a mask was used for etching of the isolation groove between the laser and modulator sections.
- (4) A thick

metalization layer was formed for high frequency performance. Finally, the device was thinned and n-type ohmic contact was deposited. An SEM picture of the cross-sectional view of the laser/modulator is shown in Figure 3.

The wafer was further cleaved into 3-mm long bars, which included the laser region, the modulator region and the isolation gap. The length for the modulator was $< 100 \mu\text{m}$. The metal pattern on the top was carefully designed in order to have high frequency operation for the modulator. The devices were bonded to a silicon carrier for RF testing.

III. DEVICE PERFORMANCE

Under room temperature, the continuous wave (CW) output power of the laser against injection current to the laser section is shown in Figure 4, with the modulator section biased at zero volts. The best devices showed a surprisingly low threshold current of 50-mA for such a long cavity length. 20-mW of single mode output power was achieved under ~ 300 -mA of driving current.

Figure 5 shows the L-I curves of the laser when different dc voltages are applied to the modulator section. The curves indicate that the laser power can be modulated by the modulator at any driving current above threshold.

Figure 6 shows the laser output power (from the single mode fiber and with 148-mA driving current), as a function of the applied voltage across the modulator. About 50% fiber coupling efficiency is obtained. The high output power of this laser/modulator would be excellent for obtaining OE oscillation.

The RF reflection and modulation response were measured with an HP8607A Lightwave Network Analyzer and are shown in Fig. 7a and 7b. As indicated in Fig. 7a, the modulation response has a sharp peak at 13.6 GHz, due to resonant enhancement. When closing the OE loop, this resonant enhancement will force the OE oscillation at 13.6 GHz and cause the laser to mode-lock. The reflection coefficient of the device is about -15 dB at 10 GHz and -8 dB at 15 GHz, which is in agreement with the design.

The mode-beating spectrum of a free running laser was observed with a photodetector directly connected to a RF spectrum analyzer and is shown in Fig. 8a. The strong mode beating at 13.6 GHz again indicates that when closing the OE loop, the COEO will be

forced to oscillate at 13.6 GHz and cause the laser to mode-lock. The RF spectrum also indicates that the laser is free of self-pulsation under the operating condition. The phase noise of the mode-beating signal was significantly reduced when a RF signal of 5 dBm at 13.6 GHz was applied to the E/A modulator, as shown in Fig. 8b. This indicates that the laser can easily be mode locked. Due to the lack of an RF filter with center frequency at 13.6 GHz at the time of experiment, we were unable to close the O/E loop and demonstrate COEO operation using this device.

SUMMARY

We have demonstrated an integrated laser/modulator (ILM) using the identical active layer approach for opto-electronic oscillator applications. The ILM device has a device length of 3-mm which results in a mode spacing of 13.6 GHz. The laser threshold current is 50-mA. Under 150 mA driving current, 5-mW of optical power has been coupled into single mode fiber. The RF performance of the ILM has been tested under this condition. Evidence of 30dB resonate enhancement has been observed for only 5dBm of microwave power applied. The full demonstration of a COEO based on the integrated laser/modulator is currently under way.

Removal of the bulky microwave components would be a key step toward on-chip integrated opto-electronic oscillator, which we believe is possible in the near future.

V. ACKNOWLEDGEMENT

The research described in this paper was performed by the Center for Space Microelectronics Technology, Jet Propulsion Laboratory, California Institute of Technology, and was sponsored by the National Aeronautics and Space Administration, Office of Space Sciences.

VI. REFERENCES

1. X. S. Yao and L. Maleki, "Converting light into spectrally pure microwave oscillation," *Optics Letters* Vol. 21 (7), pp. 483-485 (1996).
2. X. S. Yao and L. Maleki, "Optoelectronic microwave oscillator," *J. Opt. Soc. Am. B*, Vol. 13 (8), pp 1725-1735 (1996).
3. X. S. Yao and L. Maleki, "Ultra-low phase noise dual-loop optoelectronic oscillator," *OFC'98 Technical Digest*, pp.353-354 (1998).
4. X. S. Yao and L. Maleki, "Dual microwave and optical oscillator", *Optics Letters*, Vol. 22 (24), pp. 1867-1869 (1997).
5. P. Steinmann, B. Borchert, B. Stegmüller, "Improved behavior of monolithically integrated laser/modulator by modified identical active layer structure", *IEEE, Photonics Technology Letters*, vol.9, no.12, pp.1561-1563, 1997
6. W. Si, Y. Luo, D. Li, K. Zhang, Y. Nakano, K. Tada, "Analysis of distributed feedback semiconductor laser-electroabsorption modulator integrated light source, including gain-coupled structure", *Japanese Journal of Applied Physics, Part 1*, vol.34, no.2B, pp. 1260-1264, 1995.
7. D. Delprat, A. Ramdane, A. Ougazzaden, M. Morvan, and Y. Sorel, "High performance DFB laser-electroabsorption modulator based on the identical active layer approach and application to 10 Gbit/s transmission over 125 km of standard fiber", *Proc. Of 11th International Conference on Integrated Optics and Optical Fibre Communications – 23rd European Conference on Optical Communications IOOC-ECOC 97*, pp.167-170, vol.1, Sept. 22-25, 1997, Edinburgh, UK.
8. R.M. Lammert, S.D. Roh, J.S. Hughes, M.L. Osowski, and J.J. Coleman, "MQW DBR lasers with monolithically integrated external-cavity electroabsorption modulators fabricated without modification of the active region", *IEEE Photonics Technology Letters*, vol.9, no.5, pp. 566-568, 1997.

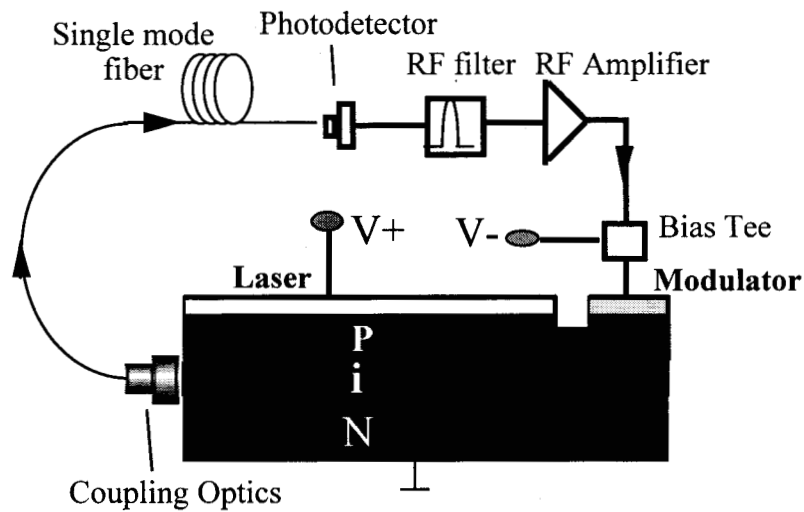
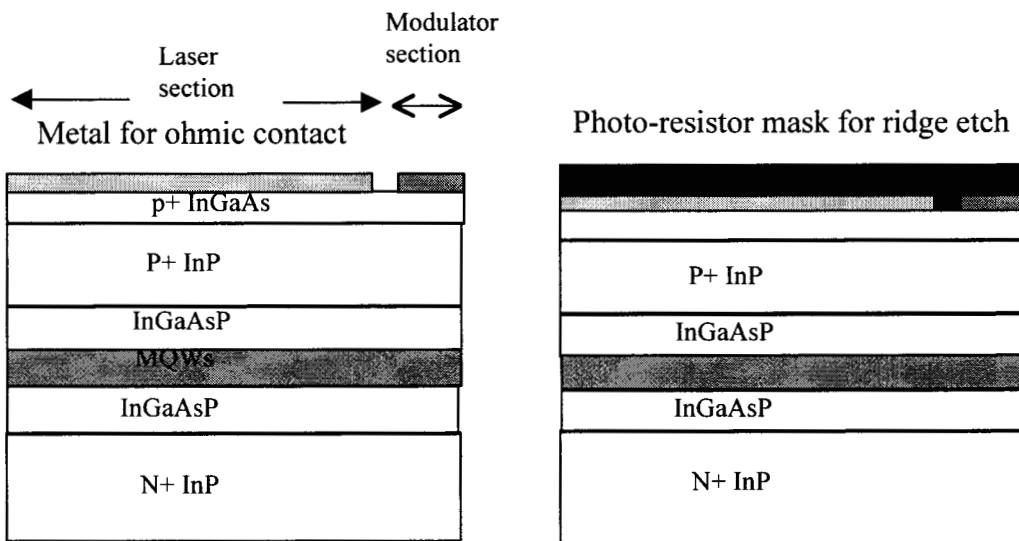


Fig. 1 Illustration of an identical active layer type laser/modulator and its application in coupled optoelectronic oscillator (COEO).



(1) Metal deposition for ohmic contact to laser section and modulator section.

(2) Photo-resistor mask for ridge etch.

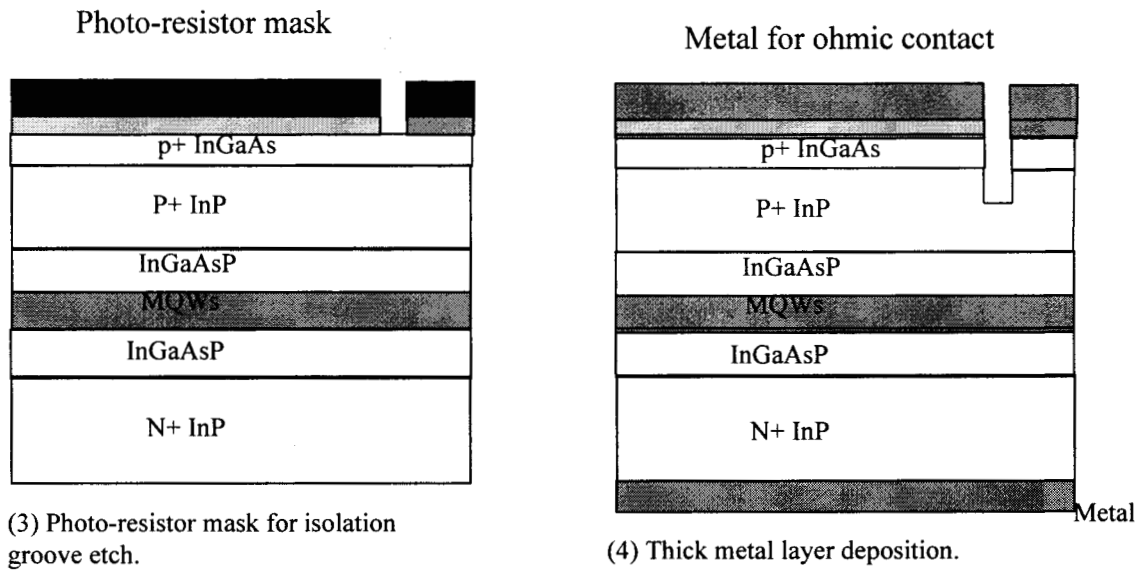


Figure 2 Fabrication processes for integrated laser/modulator.

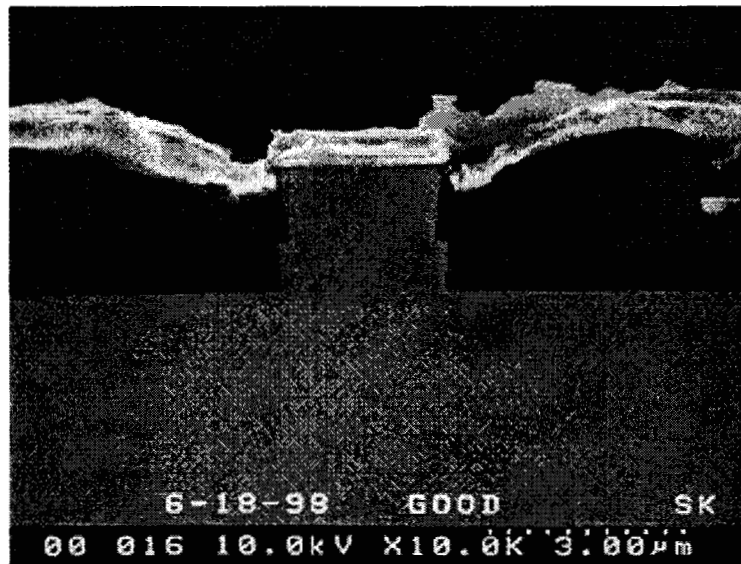


Figure 3 An SEM picture of the cross-section view of the integrated laser/modulator.

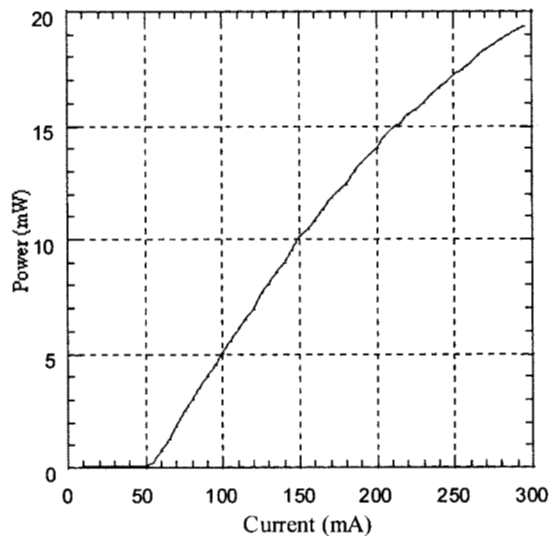


Figure 4. CW laser output power versus injection current at room temperature. During measurement, the modulator has zero bias.

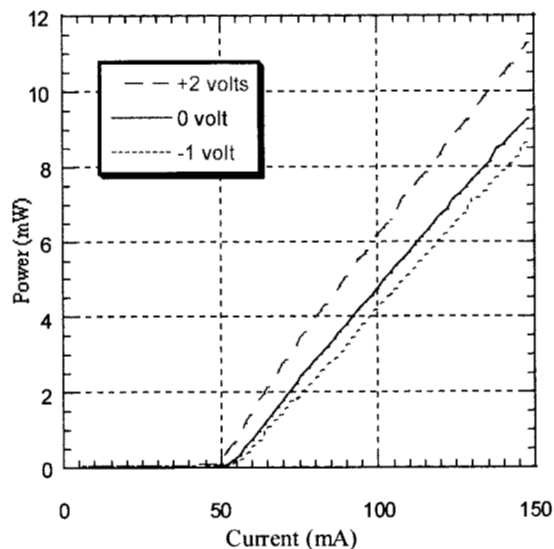


Figure 5. CW laser power versus driving current for different biased voltage applied to the modulator at room temperature

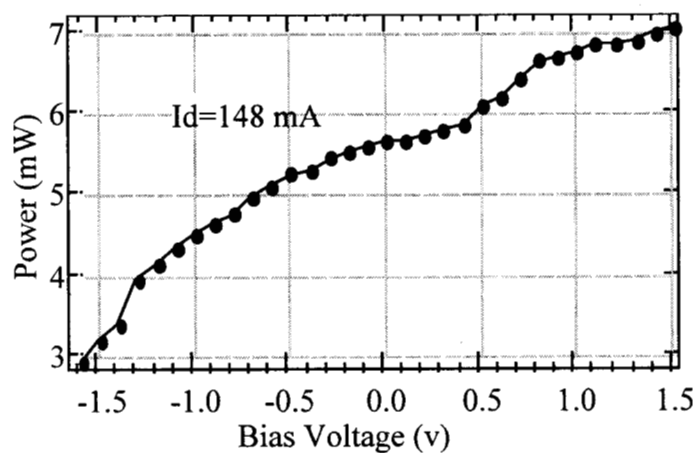


Fig. 6 The laser output power coupled into a single mode fiber as a function of bias voltage across the electro-absorption modulator.

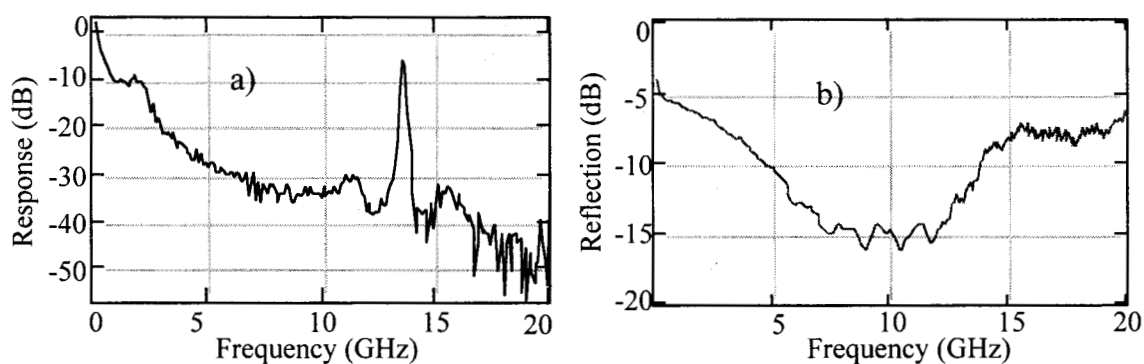


Fig. 7 a) RF response of the integrated laser/modulator. b) RF reflection coefficient of the integrated laser/modulator.

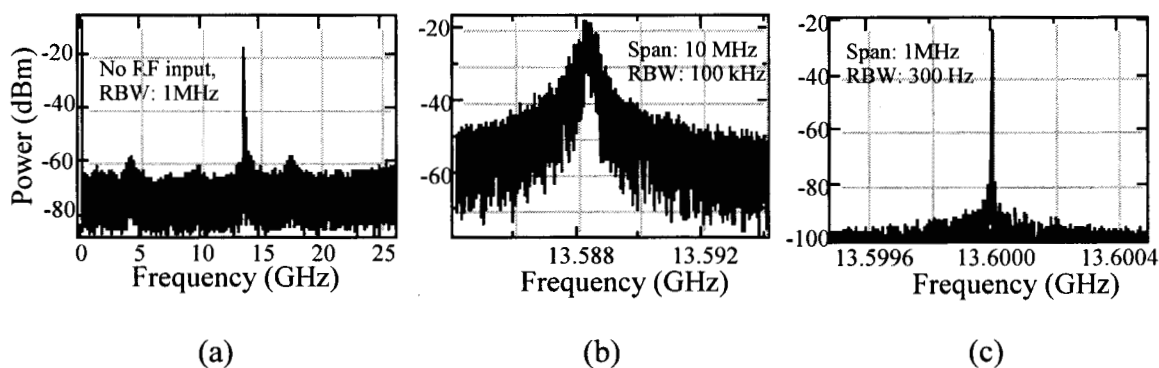


Fig. 8. a) and b) Mode-beating spectrum of a free running integrated laser/modulator for different spectrum analyzer settings. c) The mode beating spectrum of same device with a 5 dBm RF signal at 13.6 GHz applied to the modulator. Note the difference in total span and resolution bandwidth (RBW) of the spectrum analyzer settings.